Asian Journal of Health Sciences 2024, 9(2):56

Open Access Full Text Article

Original Research

An efficient UV-C device for decontaminating personal protective equipment (PPE) soiled with human Corona and Influenza virus: Solution for small-scale reuse

Aparna Varma[1], Sucharita Bhowmick[1], Afruja Khan[1], Sandeep Yadav[1], Gourav Gupta[2], Amirul Islam Mallick[1,*]

ABSTRACT

In recent times, the world has witnessed a substantial surge in the use of non-recyclable items such as Personal Protective Equipment (PPE) due to the COVID-19 pandemic. This increase has exacerbated environmental pollution levels and placed a significant strain on the global waste management system. Therefore, an effective strategy to address the logistical challenges in the demand-supply disparity and the sustainable management of used PPE is urgently needed. Through this work, we aim to develop a cost-effective, convenient, and efficient strategy to safely reuse PPE by engineering an in-house UV-C-based Sanitization Device (UVSD) and systematically evaluating its potential to disinfect virus-contaminated PPE. To this end, we have engineered a UV-C-based Sanitization Device (UVSD) and tested its ability to disinfect PPE experimentally soiled with human Influenza (A/PR/8/1934/H1N1) and human Coronavirus (HCoV-OC43) through in vitro cell culture assays. Briefly, the percentage of cell protection was determined by MTT assay, the quantification of viral gene transcript numbers was calculated by RT-qPCR, and viral titer was determined by viral plaque formation assay. Additionally, indirect immunofluorescence and viral hemagglutination assays were performed to visualize and quantify residual viral titers after UV-C irradiation. Our results demonstrate that a 15-minute exposure of virus-contaminated PPE within the UVSD cabinet can effectively inactivate both the H1N1 and HCoV-OC43 viruses, suggesting its applicability at organizational levels, including healthcare and other occupational settings.

Key words: Human Coronavirus, Human Influenza virus, UV-C decontamination, Personal Protective Equipment (PPE)

[1]*Department of Biological Sciences, Indian Institute of Science Education and Research Kolkata, Mohanpur, Nadia, West Bengal-741246, India*

[2]*Dreamz Electrical Instruments Pvt. Ltd., Salt Lake City, Kolkata - 700064, India*

Correspondence

Amirul Islam Mallick, Department of Biological Sciences, Indian Institute of Science Education and Research Kolkata, Mohanpur, Nadia, West Bengal-741246, India

Email: amallick@iiserkol.ac.in

History

- Received: Feb 14, 2023
- Accepted: Dec 28, 2023
- Published Online: Dec 31, 2023

DOI :

https://doi.org/10.15419/ajhs.v9i2.527

BioMedPress
The Open Access Publisher

INTRODUCTION

Amidst the upsurge of several infectious diseases worldwide, the twenty-first century has witnessed numerous epidemics and pandemics caused by viral, bacterial, or other pathogens, costing millions of lives. In the recent past, the H1N1 pandemic (pH1N1), caused by the Influenza Type A virus, was reported as the first pandemic of this century, followed by the WHO declaration of the recent outbreak of Coronavirus Disease 2019 (COVID-19) as a global pandemic [1–3]. Apart from these, during this time, we have also experienced several deadly episodes of epidemics in different parts of the world in the form of Zika, Ebola, Chikungunya, SARS-CoV, MERS-CoV, and the Influenza A H1N1 (pdm09) virus outbreak [3–6]. However, the recent pandemic outbreak of COVID-19, caused by severe acute respiratory syndrome-coronavirus-2 (SARS-CoV-2), has exhibited unimaginable devastation to public health and significantly impacted the global economy. While the global death toll from the COVID-19 pandemic has reached over 6 million, its occasional surge remains a significant concern [7]. The WHO has recommended several simple yet effective baseline safety and preventive measures at an individual level to combat COVID-19, including face masks, hand sanitizers, disinfectants, and maintaining social distancing in public places. Additionally, the use of Personal Protective Equipment (PPE), such as protective gowns, face masks, face shields, head covers, gloves, etc., is also considered indispensable at organizational levels, particularly for frontline health workers. Such behavioral changes have resulted in substantial demand for PPE, leading to a significant increase in its global production [8].

However, on the other side, the surge in the use of non-recyclable items, including PPE, has also increased the burden on the global waste management system with an overwhelming environmental impact, including increased total carbon footprint emissions [9–13]. Therefore, efficient, proactive measures must be in place to mitigate the challenges associated with the logistical anomalies in its manufacture-supply chain. In the search for environmentally

Cite this article : Varma A, Bhowmick S, Khan A, Yadav S, Gupta G, Mallick A I. **An efficient UV-C device for decontaminating personal protective equipment (PPE) soiled with human Corona and Influenza virus: Solution for small-scale reuse**. *Asian J. Health Sci.* 2024; 9(2):56.

friendly and sustainable management of used PPE, an increasing body of evidence supports the concept of their reuse. To this end, Ultraviolet (UV) radiation-based surface disinfection methods have attracted significant attention and gained marked visibility in the global market[14–16]. Several studies have demonstrated that UV-C radiation has the most robust genotoxic properties among the other subtypes of the UV spectrum[17]. Although the effectiveness of UV-C irradiation on the infectivity of viruses is well documented, sub-optimal or over-exposure can increase the risk of unwanted mutations, such as single-base substitutions, frameshift mutations, or small deletions. This could result in new pathogenic strains or even render the pathogens resistant to UV-C irradiation[18,19].

In addition to the adverse mutagenic effects on microbes, UV-C radiation can also aggravate several health complications in humans, including skin cancer (melanoma), lupus erythematosus, and pemphigus[20–22]. Thus, the inappropriate use and limited understanding of the correct parameters of UV-C-mediated disinfection devices engineered by commercial manufacturers may lead to vicious behavioral changes in the microbial population. Intending to uphold the beneficial use of UV-C towards limiting virus spread, in this study, we systematically evaluated the effectiveness of an in-house made UV-C sanitization device (UVSD) in decontaminating soiled PPE. We have shown that a 15-minute exposure to the virus-contaminated PPE within the UVSD cabinet could effectively inactivate the human H1N1 Influenza virus (A/PR/8/1934/H1N1) and Human Coronavirus (HCoV) OC43. Together, our results demonstrate the possible application of UV-C radiation as an effective strategy to reuse PPE in several organizational setups, including healthcare and other occupational settings.

METHODS

Cells and Viruses

Madin-Darby Canine Kidney (MDCK) cells and Vero cells were obtained from NCCS (Pune, India) and were maintained in Dulbecco's Modified Eagle's Medium (DMEM; Gibco, Thermo Fisher Scientific, USA) supplemented with 10% fetal bovine serum (FBS; Gibco, Thermo Fisher Scientific), 100 U/mL penicillin, and 100 μg/mL streptomycin (P/S; Gibco, Thermo Fisher Scientific) at 37 °C with 5% CO2 supplementation.

The Influenza Type A/PR/8/1934 (H1N1) virus was procured from ATCC (ATCC® VR-95™) and cultivated in the allantoic fluid of 10-11 day-old embryonated chicken eggs as per previously published protocols[23]. The titer of the harvested virus was calculated as the 50% Tissue Culture Infectious Dose (TCID50/mL) as per the published protocols[24,25]. Human Coronavirus OC43 (HCoV-OC43) was obtained through BEI Resources (NR-52725, NIAID, NIH, USA) and was propagated in Vero cells using DMEM supplemented with 2% FBS and P/S as per the published method[26]. After six days of infection, the virus-containing medium was harvested, and the infectivity titer of the virus was further calculated as the TCID50/mL in Vero cells.

Instrumental Design

The UVSD Cabinet is an enclosed metallic cupboard made from stainless steel with dimensions of 0.7 m × 0.9 m × 1.8 m (L × W × H). The cabinet is equipped with six Philips TUV 30W G30T8 low-pressure mercury vapor lamps, with three placed on each side of the cabinet. Each lamp emits high-power UV-C radiation with a wavelength of 254 nm. The UV-C lamps are covered with a steel mesh to ensure user safety. The cabinet is also provided with provisions for hanging PPE, other wearables, and external LED display switches for the bright light source and UV-C tubes for operation from the outside. **Figure 1**A represents the outline and proposed use of the UVSD cabinet for the present study.

Experimental Setup

Briefly, a small piece of PPE (2 × 2 cm) was cut and placed in a 35mm sterile Petri dish. The PPE used here is a 75 GSM non-laminated, disposable, single-layer, non-woven polyester-make coverall gown. Next, 12 μL of H1N1 virus sample (50 TCID50) and 60 μL of HCoV-OC43 virus sample (200 TCID50) were carefully drop-cast and spread evenly over the cut section of the PPE. The Petri dish was then covered and placed inside the UVSD cabinet positioned at 2.5 ft height. The lid of the Petri dish was then carefully removed, and the main door of the cabinet was closed. Next, the UV-C emanation was switched on using a switch fixed externally, and the timer was set for 5 minutes or 15 minutes. As a control, a similar-sized piece of PPE was drop-cast with the respective viruses and placed inside another UVSD cabinet without UV-C irradiation.

After the irradiation, fresh virus-infection medium was then added to the Petri dish containing the piece of PPE. The PPE was rinsed 4-5 times with the same medium to ensure the complete removal of any residual virus particles. Finally, the residual virus medium

Table 1: List of primers used for RT-qPCR

Target Gene	Primers	Amplicon size (bp)	Source
Influenza H1N1 M-gene universal primer	F- ATGAGTCTTCTAACCGAGGTCGAAACG R- TGGACAAAGCGTCTACGCTG	242	Kuchipudi et al., 2012)
Human Coronavirus (HCoV) OC43 N-gene universal primer	F- CCCAAGCAAACTGCTACCTCTCAG R- CGTCTGTTGTGTCTGTACCAGTACCC	188	This work

Table 2: Efficiency of H1N1 and HCoV-OC43 virus inactivation by UVSD cabinet

Virus type	Assessment method	Virus only	5 min UV-C	15 min UV-C
H1N1	% Cell protection (MDCK cells)	-	58.67±2.58**	88.39±3.38
	Viral M-gene transcript number	225.13±10.03	26.45±15.20**	0.08 ± 0.03
	HA titre	128 ± 0	6±2	Not detectable
HCoV-OC43	% Cell protection (Vero cells)	-	84.95±3.15	100.77±8.5
	Viral N-gene transcript number	$2.35x10^{11}$±$5.9x10^{10}$	3x105±$9.2x10^{4}$*	5.8x104±$1.7x10^{4}$

*Indicates significant difference between two treatment groups (5 min vs. 15 min); *P ≤ 0.05 and **P ≤ 0.01.

was collected and subjected to further assessment. A schematic representation of the experimental procedure is presented in **Figure 1**B.

Assessment of Viral (Human H1N1 Virus) Inactivation by UV-C Exposure Inside the UVSD Cabinet

The cell viability (MDCK cells) against infection with the human H1N1 virus was assessed following published protocols with slight modifications[27]. Briefly, MDCK cells were cultured at a density of 1.5 x 10^4 cells per well in standard 96-well tissue culture plates (Tarsons, India) and grown to 80% confluency at 37°C under 5% CO_2. Subsequently, the cells were infected with the treated virus (either UV-C exposed or unexposed) at 50 $TCID_{50}$. Next, the virus-containing medium was removed, the wells were washed with 1X PBS, replenished with fresh infection medium, and incubated for 48 h under 5% CO_2. The cells were then checked for morphological changes and visible cell cytopathic effects (CPEs). After 48 h of incubation, the medium was discarded, and the cells were thoroughly washed with 1X PBS. Finally, cell survivability was determined using the standard MTT (3-[4,5-dimethylthiazol-2-yl]-2,5-diphenyl tetrazolium bromide) assay, as described earlier[27]. The percent (%) protection of the cells was estimated using the following formula:

$$\%\ protection\ =\ \frac{(A-B)}{(C-B)}\ x\ 100$$

where A: absorbance value of UV-C exposed but infected cells; B: absorbance value of untreated but virus-infected cells; C: absorbance value of untreated and uninfected cells.

Characterization of Viral (Human H1N1 Virus) Plaque Phenotypes in MDCK Cells

A standard plaque formation assay was performed in MDCK cells using UV-C irradiated virus samples[24]. Briefly, approximately 1 x 10^5 cells were seeded in 12-well tissue culture plates until 90% confluency was achieved. Next, the medium was discarded, and the cells were rinsed with 1X PBS, followed by infection with UV-C exposed and unexposed viruses at 50 $TCID_{50}$, as previously described. After 2 hours, the cells were washed with 1X PBS, overlaid with fresh 0.3% (v/v) autoclaved agarose in 0.5-1 ml DMEM containing 1% BSA, 1 μg/mL TPCK-treated trypsin, and P/S per well, allowed to solidify, and incubated for 48 hours at 37 °C with 5% CO_2 supplementation. Next, the cell monolayer was fixed with 10% formaldehyde solution, followed by the removal of the agarose overlay by gentle scraping. The cells were stained with 1% (w/v) crystal violet (HiMedia) prepared in 5% ethanol for plaque visualization.

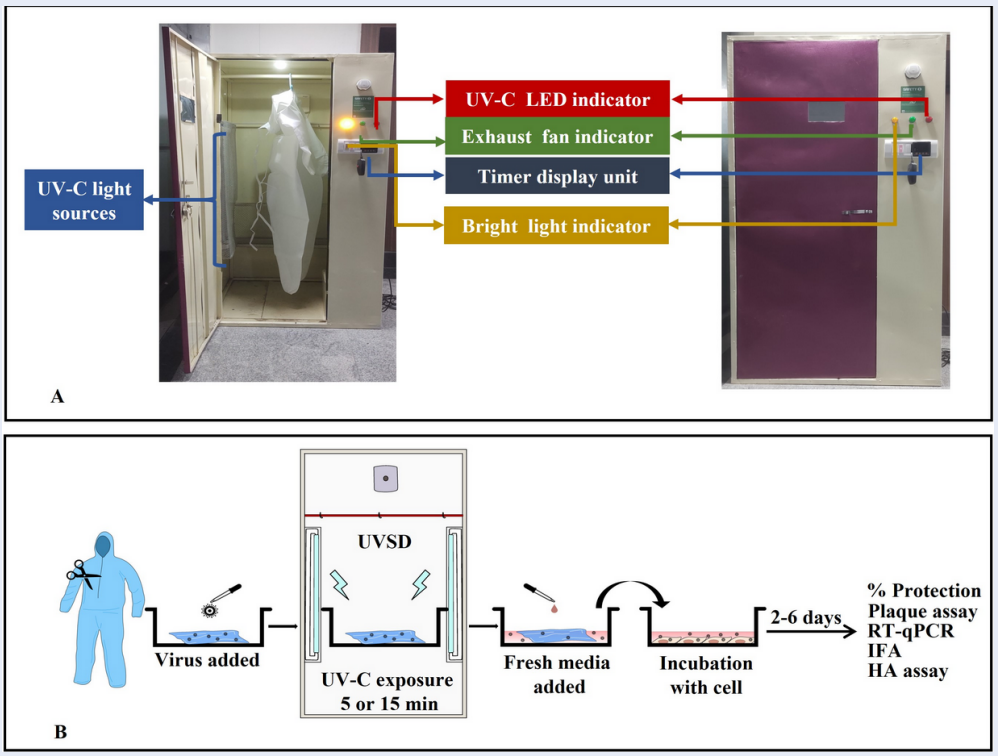

Figure 1: **SAFETY 1 UVSD cabinet operational features and schematics of the experimental setup**. (**A**) SAFETY 1 UVSD cabinet displaying different operational features. (**B**) Schematic representation of the experimental setup. A piece of the PPE (2 x 2 cm) was aseptically placed in a 35 mm petri plate. The respective amount of each of the viral particles was spread evenly on the piece of PPE. The experimentally soiled PPE piece was irradiated with UV-C inside the UVSD cabinet for 5 min and 15 min, respectively. Next, the medium containing the residual virus was collected, charged to the cells, and incubated for 48 h and 6 days, respectively, for A/PR/8/1934/H1N1 virus and HCoV-OC43 virus infection. Next, the cells were separately processed for standard MTT-based cell viability assay, Immunofluorescence assay (IFA) to detect the intracellular accumulation of infective viral particles, RT-qPCR to quantify the viral copy number, plaque reduction assay, and viral HA titration (HA assay).

Detection of Viral (Human H1N1 Virus) Nucleoprotein (NP) by Indirect Immunofluorescence Assay (IFA)

Briefly, MDCK cells were grown in 6-well tissue culture plates onto a coverslip, followed by incubation with either UV-C exposed or unexposed virus samples and monitored for the onset of visible CPEs. Next, the cells were washed with 1X PBS, fixed with 4% paraformaldehyde (PFA) for 15 minutes, treated with chilled acetone for 30 minutes, and blocked with 1% BSA solution containing 0.05% Tween-20 at 37 °C for 1 hour. The cells were then incubated with rabbit polyclonal anti-NP antibody (1:1000) (Sino Biologicals, Japan) at 4 °C overnight, then probed with FITC-labelled goat anti-rabbit IgG (Fab2, 1:1000; Thermo Fisher Scientific). After thorough washing, the cells were counterstained with 4',6-diamidino-2-phenylindole-dihydrochloride (DAPI) and fixed in VectaShield mounting media (Vector Laboratories, USA). An Olympus IX epifluorescence microscope was used for imaging, and all images were captured under 60X magnification using FITC and DAPI filters.

Quantification of Viral M Gene Copy Number by RT-qPCR

Briefly, total RNA was extracted from the virus-challenged (Human H1N1) MDCK cells using TRIzol reagent (Invitrogen, USA), followed by cDNA preparation with approximately 1000 ng of the total RNA sample using MuLV reverse transcriptase from the Superscript Reverse Transcriptase kit (BioBharati, India). For the quantitative real-time PCR (RT-qPCR), 5 μL of 2X SYBR Green PCR master mix (Applied Biosystems, USA) was combined with 2.4 μL of nuclease-free water, 0.3 μL of M gene-specific primer sets, and 2 μL of cDNA template (1:2 diluted).

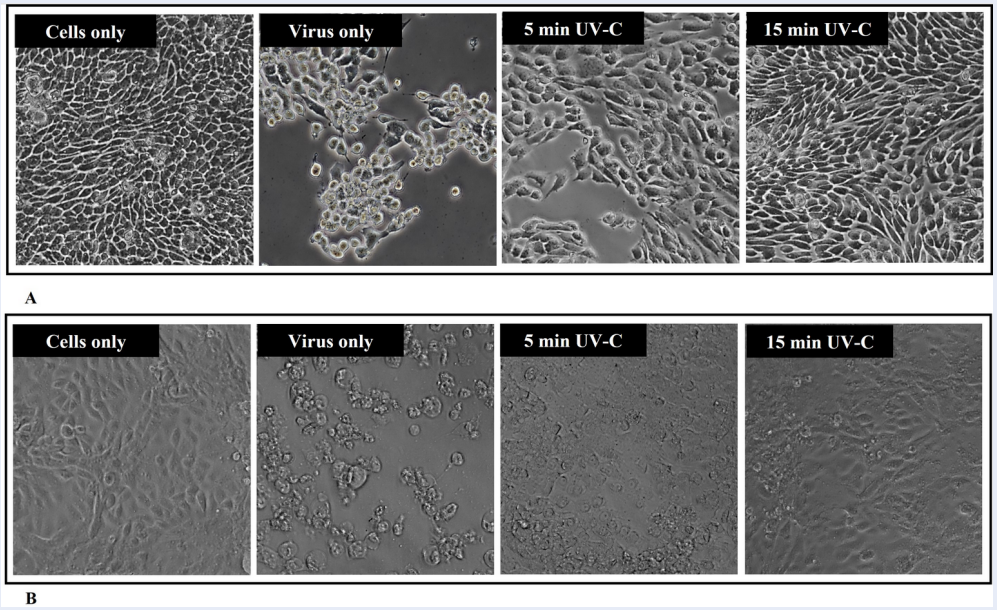

Figure 2: **Effect of UV-C exposure on MDCK and Vero cell viability against Influenza H1N1 virus (A/PR/8/1934/H1N1) and human coronavirus (HCoV-OC43)**. (**A**) Virus inactivation induced by UV-C exposure using UVSD cabinet was assessed by infection of MDCK cells with the UV-C irradiated virus samples for 5 min and 15 min. No changes in terms of CPE can be observed in the MDCK cells incubated with a virus sample UV-C exposed for 15 min inside the UVSD cabinet. Imaging was performed using Nikon TS100 inverted light microscope (Nikon, Tokyo, Japan) at 20X magnification. (**B**) Reduction in the cytopathic effects of Vero cells charged with UV-C irradiated HCoV-OC43 virus. Cells charged with the unirradiated virus are characterized by rounding up, with cytoplasmic vacuolization, sloughing, and well-detachment. Morphology of Vero cells charged with 15 min UV-C irradiated virus was nearly unaltered, indicating a significant in vitro cell protection offered by long-time UV-C irradiation.

The viral M gene transcripts were then quantified in a CFX96 real-time PCR system (Bio-Rad, USA) with the following cycling conditions: 1 cycle at 95 °C for 2 minutes; 40 cycles at 95 °C for 15 seconds and 60 °C for 1 minute. The Ct values were calculated from three independent experiments and converted into M-gene transcript numbers. The viral M gene transcript number (nmolecules) was quantified from the previously generated M-gene (242 bp) standard curve using the following equation (**Figure 4**B).

$$n_{molecules} = \frac{m_{template}\, x\, N_A}{k\, x\, N_{bases}\, x\, 10^9}$$

where, $m_{template}$ [ng]:the amount of pMD20-M gene plasmid, N_{bases} [bp]: length of the M gene (242 bp), the average mass of one base (k): 340 [Da/bp] and the Avogadro constant: N_A [mol^{-1}] [28].

Determination of Viral (Human H1N1 Virus) Hemagglutination (HA) Titer

Briefly, 1 x 10^5 MDCK cells were seeded per well of a 12-well plate and incubated with either UV-C irradiated or unirradiated virus as described previously. After 48 hours of infection, the culture medium was harvested and subjected to HA titration using standard methods described earlier [29,30]. The reciprocal of the highest dilution was calculated as HA unit per sample (HAU/100 μL) [30].

In Vitro Assessment of Viral (HCoV-OC43 Virus) Inactivation in Vero Cells

To assess the effect of UV-C irradiation on the infectivity of HCoV-OC43, Vero cells were seeded in a 96-well tissue culture plate and incubated with the UV-C exposed virus sample for 3 hours. After the incubation, the cells were gently rinsed with 1X PBS, the medium was replaced with fresh infection medium, and incubation continued for 6 days at 35 °C under 5% CO2 pressure. The changes in cell morphology were then monitored for the appearance of visible cytopathic effects (CPEs). Finally, 6 days post-infection, cell viability was determined by the standard MTT assay.

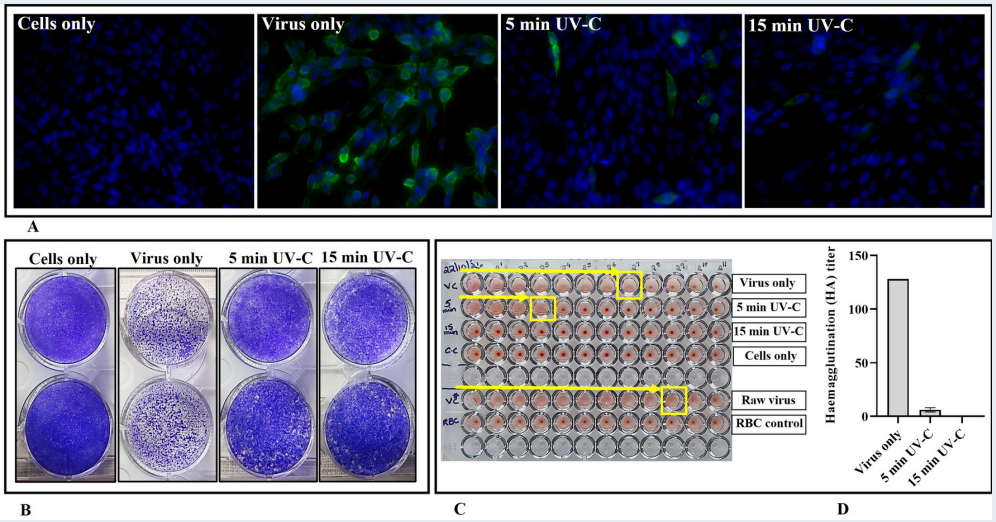

Figure 3: Reduction in accumulation of viral NP, plaque formation and HA titer of human H1N1 virus (A/PR/8/1934/H1N1). (**A**) Presence of reduced Influenza H1N1 NP protein was confirmed by immunostaining of MDCK cells infected with UV-C irradiated virus (for 5 min and 15 min). Rabbit polyclonal anti-NP antibody (1:1000) was used as the primary antibody, followed by washing and probing with FITC-labelled goat anti-rabbit IgG (Fab2, 1:1000; Thermo Fisher Scientific) as the secondary antibody for detection. Next, the cells were washed and counter-stained with 4′,6-diamidino-2-phenylindole-dihydrochloride (DAPI) for nuclear staining. Imaging was performed using Olympus 1X epifluorescence microscope under 60X magnification using FITC and DAPI filter. Green fluorescence corresponds to human H1N1 viral NP protein, and blue fluorescence corresponds to DAPI staining. Uninfected MDCK cells were taken as the positive control, while the cells infected with the virus were taken as the negative control. (**B**) Reduction in viral progeny was confirmed by standard plaque formation assay using MDCK cells. Following infection with UV-C irradiated virus sample, the cells were washed, overlayed with TPCK-trypsin supplemented 0.3 % agarose containing growth medium, and incubated for 48 h. To visualize the plaque phenotypes, the cells were then stained with 0.5 % (w/v) of crystal violet. A significant reduction in the viral plaque formation was observed when the cells were infected with UV-C exposed human H1N1 virus. (**C-D**) Determination of the HA titer of the human H1N1 virus after UV-C irradiation. Standard HA assay was performed in a U bottom 96-well plate. The sample name is marked on the right side and HA titer for each sample is highlighted in a closed box (Yellow). The HA titer was determined as the reciprocal of the highest dilution that caused complete hemagglutination of chicken RBCs. VC* indicates virus control, and RBC indicates RBC control. Images (C) and bar (D) indicate a significant reduction in the HA titer in UV-C irradiated virus sample (VC: 128 HA unit, 5 min UV-C: 8 HA unit and 15 min UV-C: undetected).

Quantification of Viral N Gene Copy Number by RT-qPCR

Total RNA from virus-infected (HCoV-OC43) Vero cells was extracted using TRIzol reagent (Invitrogen) and cDNA was synthesized. For absolute quantification of N gene transcripts, a viral N-gene (188 bp) standard curve was plotted using the pGEM-T-N recombinant plasmid (Promega, USA), and the N-gene copy number was calculated as mentioned in section 2.7 (**Figure** 4E). The number of N gene transcripts was then calculated by substituting the Ct values from all experimental test groups into the corresponding standard curve.

Statistical Analysis

Graphics and data analysis were performed using GraphPad Prism statistical software version 8.4.2 (USA). Data from RT-qPCR were analyzed using the Student's t-test (two-tailed, unpaired) to compare significant differences among the various experimental groups. The Shapiro-Wilk test was used to check the normality of each data set.

RESULTS

UV-C irradiation of human H1N1 and HCoV-OC43 viruses reduced viral infectivity

Reduction in Cytopathic Effects (CPE)

To observe the effect of UV-C irradiation on viral infectivity, we noted near-complete protection of either MDCK cells (A/PR/8/1934/H1N1) or Vero cells

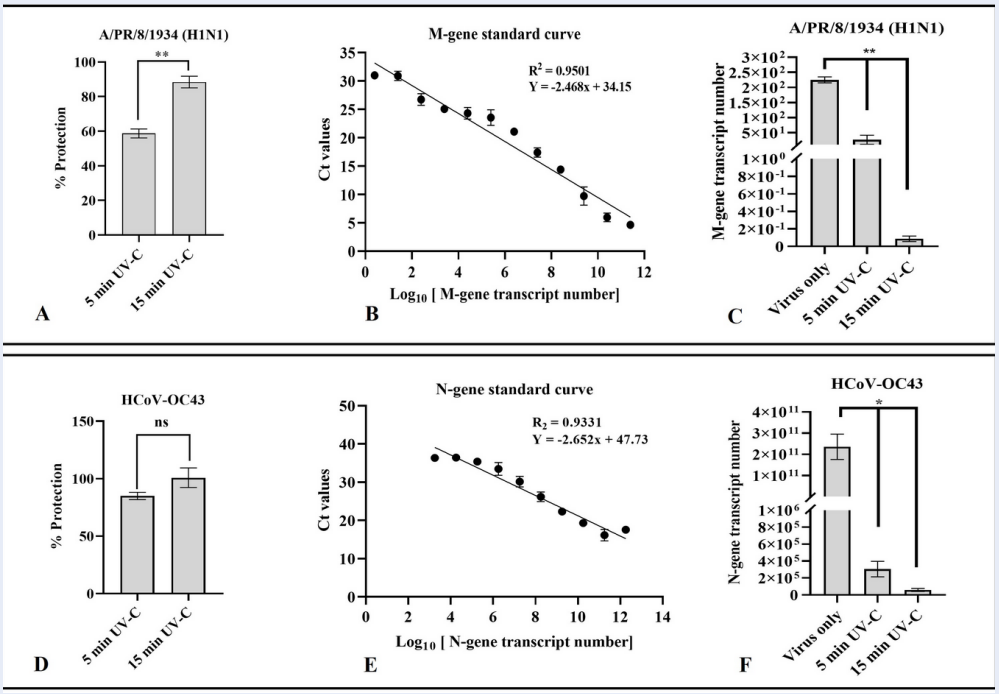

Figure 4: **Effect of UV-C irradiation on replication of human H1N1 (A/PR/8/1934/H1N1) and HCoV-OC43 virus**. (**A**) Higher cell-protective efficacy with minor CPEs was observed in MDCK cells infected with UV-C irradiated human H1N1 virus (for 5 min and 15 min) when assessed by standard MTT assay and cell viabilities were represented as the percentage (%) of cell protection. The bar indicates the mean cell protection % ± SE of three independent experiments performed in triplicates. Asterisks (*) denote statistically significant differences (*P≤ 0.05) between the two treatment groups. (**B**) Inhibitory effects of UV-C exposure on human H1N1 virus replication were confirmed by analyzing the viral M-gene transcripts. For the viral M gene standard curve generation, the Ct values (x-axis) of each dilution were plotted against the log10 of the M-gene transcript number calculated from the input number of plasmids (initial concentration ~165 ng/μL) for each dilution (y-axis). (**C**) Quantification of viral M gene transcript in MDCK cells infected with virus samples exposed to UV-C irradiation for 5 min or 15 min was performed by RT-qPCR. Each bar indicates the M-gene transcript number ± SE of two independent experiments. Asterisks (*) denote statistically significant differences (** P≤0.01) in comparison to the control (MDCK cells infected with the unirradiated virus). (**D**) Assessment of cell viabilities of virus-infected Vero cells. Higher protective efficacy with negligible CPEs was determined by standard MTT assay. Significant cell viabilities translating to a percentage (%) of cell protection were observed in cells charged with either 5 min or 15 min UV-C irradiated HCoV-OC43 virus. Each bar indicates the mean protection % ± SE of three independent experiments performed in triplicates. 'ns' indicates a statistically non-significant difference between the two treatment groups. (**E**) Viral N-gene transcript standard curve for the quantitative detections of UV-C irradiated or unirradiated viruses. Serial dilutions of pGEM-T Easy-N plasmid were analyzed by using standard amplification conditions. The Ct values (x-axis) of each dilution are plotted against the log10 of the N-gene transcript number, as calculated from the input number of plasmids (initial concentration ~ 945 ng/μL) containing the gene for each dilution (y-axis). (**F**) Quantification of viral N gene transcript in Vero cells charged with either 5 min or 15 min UV-C irradiated virus. Replication of viral RNA was determined by RT-qPCR using gene-specific primers. Each bar indicates the N-gene transcript number ± SE of two independent experiments performed in duplicates. Asterisks (*) denote statistically significant differences (* P≤0.05) in comparison to the control (virus-only) group.

(HCoV-OC43), except for a few lesions indicating cytopathic effects (CPE). This observation was evident when the virus sample, collected from the contaminated PPE, was exposed for 15 minutes inside the UVSD cabinet. However, characteristic changes such as cell rounding, condensation, and shrinkage were visible when the virus sample was exposed to UV-C for 5 minutes (**Figure 2** A, B).

Enhanced Protection of MDCK or Vero Cells Against H1N1 or HCoV-OC43 Virus

More than 90% cell survivability was confirmed by a standard MTT assay when the virus sample was irradiated for 15 minutes. In contrast, only 50% cell survivability could be achieved if exposed for 5 minutes inside the UVSD cabinet. This observation was consistent for both human H1N1 and HCoV-OC43 viruses, suggesting effective viral inactivation after 15 minutes of UV-C irradiation (**Figure 4** A, D).

Reduction in Viral (Human H1N1 Virus) Plaque Formation

A standard plaque assay was performed on MDCK cells against the human H1N1 virus to directly assess the residual infectivity of the UV-C irradiated virus. As shown in Figure 3B, a significant reduction in viral plaques for the samples exposed for 5 and 15 minutes of UV-C irradiation was observed.

Reduction in Viral (Human H1N1 Virus) NPs in MDCK Cells

The ability of UV-C exposure to inhibit viral replication was assessed through an IFA, and the presence of viral NPs in the infected MDCK cells was determined. In line with our observation from the plaque assay, the current data suggest a minor accumulation of viral NP protein, particularly when MDCK cells were charged with virus irradiated for 15 minutes inside the UVSD cabinet. However, comparatively higher signals were detected for the 5-minute exposure, indicating incomplete inactivation of the virus (**Figure 3** A).

Transcriptional Analysis of Viral M (Human H1N1) or N (HCoV-OC43) Gene Transcripts

To observe the effect of UV-C irradiation on viral replication, viral M-gene (for human H1N1 virus) or N-gene (for HCoV-OC43) transcripts were quantified by RT-qPCR (**Table 1**). Compared to the respective standards, a significantly low number of viral transcripts ($P \leq 0.01$ for human H1N1; $P \leq 0.05$ for HCoV-OC43) were observed for both viruses that received UV-C exposure for 15 minutes (**Figure 4** C, F). In contrast to the 15-minute UV-C exposure, although a considerable reduction in viral M or N gene transcript was noted when 5-minute UV-C exposure was given, the reduction was significantly less compared to 15 minutes of exposure.

Reduction in Viral HA Titer (Human H1N1 Virus)

To assess the residual infectivity of the UV-C irradiated human H1N1 virus, when titrated for viral HA units, we observed an absolute reduction in HA titer in the case of 15 minutes of UV-C exposure. However, the reduction was found to be 16-fold in the case of 5 minutes exposure (128 HA to 8 HA) (**Figure 3** C, D).

DISCUSSION

The recent outbreak of the COVID-19 pandemic has increased the demand for single-use PPE worldwide, particularly in organizational setups such as primary healthcare settings, airline services, and lodging services[31–33]. However, within a short period, to meet the adequate supply, large-scale industrial production has led to the indiscriminate use of PPE, resulting in a substantial increase in plastic waste. These single-use plastics can degrade into smaller particles of around 5 mm under normal environmental conditions, making them a potential source of microplastic fibers[34]. Hence, considering the logistical anomaly in demand versus supply and the adverse impact on the environment, a convenient and cost-effective approach is needed to ensure an uninterrupted supply of PPE without additional burden on our waste disposal system.

To address this issue, the germicidal value of UV radiation has gained significant global attention. Historically, UV-based disinfection methods are well-perceived and have been in practice for a long time, particularly in the healthcare sector, pharmaceutical industries, and research establishments[35–37]. UV germicidal irradiation (UVGI) is the region in the UV spectrum that corresponds to the UV-C wavelength range of 200-280 nm[35]. It has been reported that UV radiation penetrates the cell membrane of microbes, leading to the formation of intra-strand cyclobutyl pyrimidine dimers between adjacent pyrimidine residues in their nucleic acid molecules[35,37–39]. These dimers are eventually read as a single base during the subsequent replication cycles by DNA polymerase, resulting in frameshift mutations and impairing their replication[37,39,40].

This study aimed to establish the efficacy of an in-house-made UVSD cabinet in disinfecting virus-contaminated PPE. The UVSD cabinet used in this study is equipped with six commercially available Philips TUV 30W G30T8 low-pressure mercury vapor lamps that emit high-power UV-C radiation and are commonly used in residential and industrial air and water disinfection systems.

Given that the pandemic potential of an RNA virus is higher than that of DNA viruses, we chose to use two single-stranded RNA viruses, namely the human H1N1 virus and HCoV-OC43, for the current study. Considering the safety and other restrictions of using the SARS-CoV-2 virus, we decided to use a human beta coronavirus, HCoV-OC43, as a surrogate of the SARS-CoV-2 virus[41].

Although the receptors are different, the human H1N1 and HCoV-OC43 viruses affect the respiratory tract and cause mild to severe pneumonia in humans. Moreover, respiratory droplets are the primary transmission mode for both viruses with exceptionally long environmental persistence[42–45]. This has mainly been observed in healthcare settings where disposable PPE poses a significant risk of pathogen transmission and forfeits its safety without decontamination before disposal.

To rationalize the safe reuse of PPE, we have shown that UV-C irradiation of contaminated PPE for 15 minutes inside the UVSD cabinet can effectively reduce the infectivity of both the human H1N1 and HCoV-OC43 virus (**Table 2**). For the human H1N1 virus, the efficacy of the UVSD cabinet was assessed in terms of reduction in CPEs, percent cell survivability, quantification of viral M gene transcript numbers, and titration of residual HA units present in the UV-C irradiated samples. Our results suggest that UV-C treatment for 15 minutes can significantly reduce the viral infectivity of the host cells. Since the mutation of the influenza A viral Ribonucleoprotein (vRNP) and Nucleoprotein-Nuclear Export Signal (NP-NES) are responsible for impaired viral replication, we next performed an IFA to see if UV-C irradiation affects vRNP complexes[46–48]. Our data indicate that 15 minutes of UV-C exposure to the human H1N1 virus substantially reduces viral replication potential and limits the productive accumulation of infectious viral particles inside the cells. Given that the HA surface glycoprotein of the influenza virus plays a critical role in viral entry and fusion to host cells, further, we claim that UV-C exposure to contaminated PPE for 15 minutes can ensure an absolute reduction in HA titer[49–51]. Finally, the data obtained from transcriptional analysis of the influenza M gene segment indicates the potential of UV-C irradiation in limiting the intracellular accumulation of vRNA.

Next, we tested the efficacy of the present module against the HCoV-OC43, and it was found that, similar to H1N1 infection, a significant drop in viral infectivity was also observed in Vero cells. To determine the temporal relationship between residual viral infectivity and viral copy number, RT-qPCR of the viral N gene segment was performed, and the results indicated an effective impairment of viral transcription and replication machinery by UV-C exposure.

Considering the public health implication of the COVID-19 pandemic, the use of viral inactivation systems, including UV-C-based disinfection practices, is expected to grow in the coming days. However, given that UV-C light sources are based on mercury for their high-energy radiation emission, the mass adoption of such devices may pose an intrinsic environmental threat[52,53]. To this end, several alternative discharge lamps are currently available on the market, such as ultraviolet light-emitting diodes (LEDs) and aluminum gallium nitride (AlGaN) material-based deep ultraviolet LEDs. Although they are less efficient compared to low-pressure mercury lamps, low voltage operation, quicker turn-ons, and compactness make them an appropriate alternative[53]. Recently, it has also been reported that the efficacy of UV-C disinfection primarily depends on the PPE materials, not on their shape[54]. Therefore, we expect that the UVSD cabinet used in the present study can be useful for sanitizing some models of complex PPE if the intensity of UV-C irradiation and exposure time is optimized.

Another critical factor that needs to be considered is the ability of the PPE material to endure the UV-C radiation and maintain its integrity and quality for possible future reuse. Several studies have investigated the effect of UV-C radiation on N95 and surgical masks, but its impact on the surface integrity of PPE gowns has not been thoroughly studied[54–57]. The PPE material used for the present study is made from non-woven polyester 75-GSM fibers. In contrast to woven fibers, non-woven polyester does not allow the virus inoculum to penetrate the inner layers. Instead, it remains adsorbed onto the outer surface of the PPE, making the virus particles more exposed to UV-C irradiation[58,59].

Thus, while the efficacy and performance of the UVSD could be further optimized and validated, we demonstrated its reliability and efficiency in its potential for decontaminating PPE and other common wearables. We also claim that UV-C exposure of viral particles in

the UVSD is safe, less time-consuming, and hazard-free compared to other techniques like fumigation or chemical sterilization, thus making it more suitable for possible application in different organizational setups.

CONCLUSIONS

Considering the role of UV-C-based disinfection strategy in controlling virus spread, the in-house-made UVSD cabinet that was used for this study provides a robust, cost-effective, and environment-friendly approach to mitigate the increasing demand for PPE through its safe reuse. However, since the UV-C tolerance of PPE materials depends primarily on the intensity and duration of UV-C exposure, the impact of repeated UV-C irradiation and the number of possible reuses must be further evaluated.

ABBREVIATIONS

BSA - Bovine Serum Albumin, **CPE** - Cytopathic Effect, **COVID-19** - Coronavirus Disease 2019, **DAPI** - 4',6-diamidino-2-phenylindole, **DMEM** - Dulbecco's Modified Eagle's Medium, **FBS** - Fetal Bovine Serum, **GSM** - Grams per Square Meter, **H1N1** - Hemagglutinin Type 1 and Neuraminidase Type 1, **HA** - Hemagglutination, **HCoV-OC43** - Human Coronavirus OC43, **IFA** - Indirect Immunofluorescence Assay, **LED** - Light Emitting Diode, **MDCK** - Madin-Darby Canine Kidney, **MTT** - Methylthiazolyldiphenyl-tetrazolium bromide, **NP** - Nucleoprotein, **PBS** - Phosphate Buffered Saline, **PFA** - Paraformaldehyde, **PPE** - Personal Protective Equipment, **P/S** - Penicillin/Streptomycin, **RT-qPCR** - Reverse Transcription Quantitative Polymerase Chain Reaction, **TPCK** - Tosyl Phenylalanyl Chloromethyl Ketone, **UV-C** - Ultraviolet C, **UVSD** - UV-C-based Sanitization Device, **WHO** - World Health Organization

ACKNOWLEDGMENTS

AV thanks the Council of Scientific & Industrial Research (CSIR) and, SB and AK thank the University Grants Commission (UGC), Ministry of Education, Government of India for their research fellowships. We acknowledge the Central Imaging Facility at the Indian Institute of Science Education and Research (IISER) Kolkata, India, for the necessary support.

AUTHOR'S CONTRIBUTIONS

Conception and design of the study: Dr. AIM, GG; Acquisition of data (laboratory or clinical) : AV, SB, AK, SY; Data Analysis and/or interpretation: AV, SB; Drafting Manuscript and/or critical revision: AV, SY, AIM; Approval of a final version of manuscript: AV, SB, AK, SY, GG and AIM. All authors read and approved the final manuscript.

FUNDING

AIM acknowledges the financial support from M/s Dreamz Electrical Instruments Pvt. Ltd., Salt Lake City, Kolkata, India (Grant no: AM-2020-003) and IISER Kolkata Institute Research Fund.

AVAILABILITY OF DATA AND MATERIALS

Data generated or analyzed in the present study are included in this published article.

ETHICS APPROVAL AND CONSENT TO PARTICIPATE

Not applicable.

CONSENT FOR PUBLICATION

Not applicable.

COMPETING INTERESTS

The authors declare that they have no competing interests.

REFERENCES

1. Centers for Disease Control and Prevention. 2009 H1N1 Flu Pandemic Timeline [Internet]. 2019 [cited 2022 May 22]. Available from: https://www.cdc.gov/flu/pandemic-resources/2009-pandemic-timeline.html;.
2. World Health Organization. Timeline: WHO's COVID-19 response [Internet]. [cited 2022 May 22]. Available from: https://www.who.int/emergencies/diseases/novel-coronavirus-2019/interactive-timeline;.
3. da Costa VG, Saivish MV, Santos DER, de Lima Silva RF, Moreli ML. Comparative epidemiology between the 2009 H1N1 influenza and COVID-19 pandemics. Journal of Infection and Public Health. 2020;13(12):1797–804. doi:10.1016/j.jiph.2020.10.019 PMID: 33190962;.
4. Arabi YM, Balkhy HH, Hayden FG, Bouchama A, Luke T, Baillie JK, et al. Middle East Respiratory Syndrome [Internet]. 2017 [cited 2021 Oct 22]. Available from: https://www.nejm.org/doi/10.1056/NEJMsr1408795 doi:10.1056/NEJMsr1408795;.
5. Fouchier RAM, Kuiken T, Schutten M, van Amerongen G, van Doornum GJJ, van den Hoogen BG, et al. Koch's postulates fulfilled for SARS virus. Nature. 2003;423(6937):240. doi:10.1038/nature01588 PMID: 12748634;.
6. Murhekar M, Mehendale S. The 2015 influenza A (H1N1) pdm09 outbreak in India. Indian Journal of Medical Research. 2016;143(6):821–3. doi:10.4103/0971-5916.191804 PMID: 27748299;.
7. World Health Organization. WHO Coronavirus (COVID-19) Dashboard [Internet]. [cited 2022 May 22]. Available from: https://covid19.who.int;.
8. Saini V, Sikri K, Batra SD, Kalra P, Gautam K. Development of a highly effective low-cost vaporized hydrogen peroxide-based method for disinfection of personal protective equipment for their selective reuse during pandemics. Gut Pathogens. 2020;12(1):29. doi:10.1186/s13099-020-00374-7 PMID: 32817706;.

9. Bhatia P, Cummis C, Draucker L, Rich D, Lahd H, Brown (WBCSD) A. Greenhouse Gas Protocol Product Life Cycle Accounting and Reporting Standard. 2011 [cited 2021 Nov 14]. Available from: https://www.wri.org/research/greenhouse-gas-protocol-product-life-cycle-accounting-and-reporting-standard;.
10. Patrício Silva AL, Prata JC, Walker TR, Duarte AC, Ouyang W, Barcelò D, et al. Increased plastic pollution due to COVID-19 pandemic: Challenges and recommendations. Chemical Engineering Journal. 2021;405:126683. doi:10.1016/j.cej.2020.126683;.
11. Prata JC, Silva ALP, Walker TR, Duarte AC, Rocha-Santos T. COVID-19 Pandemic Repercussions on the Use and Management of Plastics. Environmental Science & Technology. 2020;54(13):7760–5. doi:10.1021/acs.est.0c02178 PMID: 32476422;.
12. Rizan C, Reed M, Bhutta MF. Environmental impact of personal protective equipment distributed for use by health and social care services in England in the first six months of the COVID-19 pandemic. Journal of the Royal Society of Medicine. 2021;114(5):250–63. doi:10.1177/01410768211003340 PMID: 33750289;.
13. Usubharatana P. CARBON FOOTPRINTS OF RUBBER PRODUCTS SUPPLY CHAINS (FRESH LATEX TO RUBBER GLOVE). Applied Ecology and Environmental Research. 2018;16(2):1639–57. doi:10.15666/aeer/1602_16391557;.
14. Bhardwaj SK, Singh H, Deep A, Khatri M, Bhaumik J, Kim KH, et al. UVC-based photoinactivation as an efficient tool to control the transmission of coronaviruses. Science of the Total Environment. 2021;792:148548. doi:10.1016/j.scitotenv.2021.148548 PMID: 34118684;.
15. Casini B, Tuvo B, Cristina ML, Spagnolo AM, Totaro M, Baggiani A, et al. Evaluation of an Ultraviolet C (UVC) Light-Emitting Device for Disinfection of High Touch Surfaces in Hospital Critical Areas. International Journal of Environmental Research and Public Health. 2019;16(19):3572. doi:10.3390/ijerph16193572 PMID: 31561483;.
16. García de Abajo FJ, Hernández RJ, Kaminer I, Meyerhans A, Rosell-Llompart J, Sanchez-Elsner T. Back to Normal: An Old Physics Route to Reduce SARS-CoV-2 Transmission in Indoor Spaces. ACS Nano. 2020;14(7):7704–13. doi:10.1021/acsnano.0c04596 PMID: 32525657;.
17. Trevisan A, Piovesan S, Leonardi A, Bertocco M, Nicolosi P, Pelizzo MG, et al. Unusual High Exposure to Ultraviolet-C Radiation. Photochemistry and Photobiology. 2006;82(4):1077. doi:10.1562/2006-02-27-IR-832 PMID: 16764446;.
18. Norval M. The effect of ultraviolet radiation on human viral infections. Photochemistry and Photobiology. 2006;82(6):1495–504. doi:10.1562/2006-06-16-IR-956 PMID: 16948706;.
19. Norval M, El-Ghorr A, Garssen J, Loveren H. The effects of ultraviolet light irradiation on viral infections. British Journal of Dermatology. 1994;130(6):693–700. doi:10.1111/j.1365-2133.1994.tb03417.x PMID: 8014563;.
20. Barbhaiya M, Costenbader KH. Ultraviolet radiation and systemic lupus erythematosus. Lupus. 2014;23(6):588–95. doi:10.1177/0961203314522337 PMID: 24567211;.
21. Glanz K, Buller DB, Saraiya M. Reducing ultraviolet radiation exposure among outdoor workers: State of the evidence and recommendations. Environmental Health. 2007;6:22. doi:10.1186/1476-069X-6-22 PMID: 17686157;.
22. Narayanan DL, Saladi RN, Fox JL. Review: Ultraviolet radiation and skin cancer. International Journal of Dermatology. 2010;49(9):978–86. doi:10.1111/j.1365-4632.2010.04474.x PMID: 20883404;.
23. Woolcock PR. Avian influenza virus isolation and propagation in chicken eggs. Methods in Molecular Biology. 2008;436:35–46. doi:10.1007/978-1-59745-279-3_3 PMID: 18369922;.
24. Lahiri A, Bhowmick S, Sharif S, Mallick AI. Pre-treatment with chicken IL-17A secreted by bioengineered LAB vector protects chicken embryo fibroblasts against Influenza Type A Virus (IAV) infection. Molecular Immunology. 2021;140:106–19. doi:10.1016/j.molimm.2021.02.018 PMID: 33640656;.
25. Reed LJ, Muench H. A SIMPLE METHOD OF ESTIMATING FIFTY PER CENT ENDPOINTS. American Journal of Epidemiology. 1938;27(3):493–7. No DOI available.;.
26. Hu Y, Ma C, Szeto T, Hurst B, Tarbet B, Wang J. Boceprevir, Calpain Inhibitors II and XII, and GC-376 have broad-spectrum antiviral activity against coronaviruses. ACS Infectious Diseases. 2021;7(3):586-97.;.
27. Lahiri A, Sharif S, Mallick AI. Intragastric delivery of recombinant Lactococcus lactis displaying ectodomain of influenza matrix protein 2 (M2e) and neuraminidase (NA) induced focused mucosal and systemic immune responses in chickens. Molecular Immunology. 2019;114:497-512.;.
28. Frensing T, Kupke SY, Bachmann M, Fritzsche S, Gallo-Ramirez LE, Reichl U. Influenza virus intracellular replication dynamics, release kinetics, and particle morphology during propagation in MDCK cells. Applied Microbiology and Biotechnology. 2016;100:7181-92.;.
29. Killian ML. Hemagglutination assay for influenza virus. Methods in Molecular Biology. 2014;1161:3-9.;.
30. Spackman E, editor. Animal influenza virus: Methods and protocols [Internet]. New York, NY: Springer US; 2020 [cited 2021 Nov 11]. Available from: http://link.springer.com/10.1007/978-1-0716-0346-8;.
31. Paterlini M. On the front lines of coronavirus: the Italian response to covid-19. BMJ. 2020;368:m1065.;.
32. Wong J, Goh QY, Tan Z, Lie SA, Tay YC, Ng SY, et al. Preparing for a COVID-19 pandemic: a review of operating room outbreak response measures in a large tertiary hospital in Singapore. Canadian Journal of Anaesthesia. 2020;1-14.;.
33. Cohen J, Rodgers Y van der M. Contributing factors to personal protective equipment shortages during the COVID-19 pandemic. Preventive Medicine. 2020;141:106263.;.
34. Fadare OO, Okoffo ED. Covid-19 face masks: A potential source of microplastic fibers in the environment. Science of the Total Environment. 2020;737:140279.;.
35. Kowalski W. Ultraviolet Germicidal Irradiation Handbook: UVGI for Air and Surface Disinfection [Internet]. Berlin, Heidelberg: Springer-Verlag; 2009 [cited 2021 Oct 22]. Available from: https://www.springer.com/gp/book/9783642019982;.
36. Kowalski W. Ultraviolet Germicidal Irradiation Handbook: UVGI for Air and Surface Disinfection [Internet]. Berlin, Heidelberg: Springer Berlin Heidelberg; 2009 [cited 2021 Nov 13]. Available from: http://link.springer.com/10.1007/978-3-642-01999-9;.
37. McKeen L. Introduction to food irradiation and medical sterilization. In: Effective sterilization of plastics and elastomers. 2012;1-40.;.
38. Heßling M, Hönes K, Vatter P, Lingenfelder C. Ultraviolet irradiation doses for coronavirus inactivation – review and analysis of coronavirus photoinactivation studies. GMS Hygiene and Infection Control. 2020;15:Doc08.;.
39. Tseng CC, Li CS. Inactivation of virus-containing aerosols by ultraviolet germicidal irradiation. Aerosol Science and Technology. 2005;39(12):1136-42.;.
40. Brickner PW, Vincent RL, First M, Nardell E, Murray M, Kaufman W. The application of ultraviolet germicidal irradiation to control transmission of airborne disease: bioterrorism countermeasure. Public Health Reports. 2003;118(2):99-114.;.
41. Schirtzinger EE, Kim Y, Davis AS. Improving human coronavirus OC43 (HCoV-OC43) research comparability in studies using HCoV-OC43 as a surrogate for SARS-CoV-2. Journal of Virological Methods. 2022;299:114317.;.
42. Casanova L, Rutala WA, Weber DJ, Sobsey MD. Coronavirus survival on healthcare personal protective equipment. Infection Control and Hospital Epidemiology. 2010;31(5):560-1.;.
43. Cook BWM, Cutts TA, Nikiforuk AM, Poliquin PG, Court DA, Strong JE, et al. Evaluating environmental persistence and disinfection of the Ebola virus Makona variant. Viruses. 2015;7(4):1975-86.;.
44. Coulliette AD, Perry KA, Edwards JR, Noble-Wang JA. Per-

sistence of the 2009 pandemic influenza A (H1N1) virus on N95 respirators. Applied and Environmental Microbiology. 2013;79(7):2148-55.;.
45. Flerlage T, Boyd DF, Meliopoulos V, Thomas PG, Schultz-Cherry S. Influenza virus and SARS-CoV-2: pathogenesis and host responses in the respiratory tract. Nature Reviews Microbiology. 2021;19(7):425-41.;.
46. Neumann G, Hughes MT, Kawaoka Y. Influenza A virus NS2 protein mediates vRNP nuclear export through NES-independent interaction with hCRM1. EMBO Journal. 2000;19(24):6751-8.;.
47. O'Neill RE, Talon J, Palese P. The influenza virus NEP (NS2 protein) mediates the nuclear export of viral ribonucleoproteins. EMBO Journal. 1998;17(1):288-96.;.
48. Stegmann T, White JM, Helenius A. Intermediates in influenza-induced membrane fusion. EMBO Journal. 1990;9(13):4231-41.;.
49. Lauster D, Glanz M, Bardua M, Ludwig K, Hellmund M, Hoffmann U, et al. Multivalent peptide-nanoparticle conjugates for influenza-virus inhibition. Angewandte Chemie International Edition in English. 2017;56(21):5931-6.;.
50. Lin Z, Li Y, Guo M, Xu T, Wang C, Zhao M, et al. The inhibition of H1N1 influenza virus-induced apoptosis by silver nanoparticles functionalized with zanamivir. Royal Society of Chemistry Advances. 2017;7(2):742-50.;.
51. Luo M, Wu X, Li Y, Guo F. Synthesis of four pentacyclic triterpene–sialylglycopeptide conjugates and their affinity assays with hemagglutinin. Molecules. 2021;26(4):895.;.
52. Hylander LD, Goodsite ME. Environmental costs of mercury pollution. Science of the Total Environment. 2006;368(1):352-70.;.
53. Trivellin N, Piva F, Fiorimonte D, Buffolo M, De Santi C, Orlandi VT, et al. UV-based technologies for SARS-CoV-2 inactivation: status and perspectives. Electronics. 2021;10(14):1703.;.
54. Golovkine GR, Roberts AW, Cooper C, Riano S, DiCiccio AM, Worthington DL, et al. Practical considerations for Ultraviolet-C radiation mediated decontamination of N95 respirator against SARS-CoV-2 virus. Public Library of Science ONE. 2021;16(10):e0258336.;.
55. Ozog DM, Sexton JZ, Narla S, Pretto-Kernahan CD, Mirabelli C, Lim HW, et al. The effect of ultraviolet C radiation against different N95 respirators inoculated with SARS-CoV-2. International Journal of Infectious Diseases. 2020;100:224-9.;.
56. Peters A, Palomo R, Ney H, Lotfinejad N, Zingg W, Parneix P, et al. The COVID-19 pandemic and N95 masks: reusability and decontamination methods. Antimicrobial Resistance and Infection Control. 2021;10:83.;.
57. Huber T, Goldman O, Epstein AE, Stella G, Sakmar TP. Principles and practice for SARS-CoV-2 decontamination of N95 masks with UV-C. Biophysical Journal. 2021;120(14):2927-42.;.
58. Karim N, Afroj S, Lloyd K, Oaten LC, Andreeva DV, Carr C, et al. Sustainable Personal Protective Clothing for Healthcare Applications: A Review. ACS Nano. 2020;14(10):12313-40.;.
59. Lindsley WG, Martin SB, Thewlis RE, Sarkisian K, Nwoko JO, Mead KR, et al. Effects of Ultraviolet Germicidal Irradiation (UVGI) on N95 Respirator Filtration Performance and Structural Integrity. Journal of Occupational and Environmental Hygiene. 2015;12(8):509-17.;.